Materials Research Proceedings 41 (2024) 678-687 https://doi.org/10.21741/9781644903131-75

Prediction of the microstructure evolution during the friction stir extrusion of a AA6061 aluminum alloy

BOCCHI Sara[1,a*], NEGOZIO Marco[2,b], GIARDINI Claudio[1,c], DONATI Lorenzo[3,d]

[1] Department of Management, Information and Production Engineering, University of Bergamo, Via Pasubio 7/b, Dalmine (BG), Italy

[2] University of Parma - Department of Engineering and Architecture, Parco Area delle Scienze, 181/A, 43124 Parma, Italy

[3] DIN Department of Industrial Engineering – University of Bologna,

Viale Risorgimento 2, 40136, Bologna, Italy

[a]sara.bocchi@unibg.it, [b] marco.negozio@unipr.it, [c]claudio.giardini@unibg.it, [d]l.donati@unibo.it

Keywords: Friction Stir Extrusion, FEM, Recrystallization, Process Sustainability, AA6XXX

Abstract. In recent years, the development of Friction Stir Extrusion (FSE) simulation models becomes crucial for gaining a deeper understanding of its underlying physics. Concurrently, there is a demand for precise control over the microstructure evolution of aluminum alloy extruded profiles, given its substantial impact on mechanical properties. Despite this, the relationship between process parameters and the evolution of grain structure remains insufficiently understood. In this context, a Lagrangian approach was established to simulate the FSE process, utilizing the commercial software DEFORM™ 3D. This research involved the investigation of the impact of various process parameters, such as rotational and descent tool speeds, on the occurrence of bonding phenomena, while considering both thermal and stress conditions. Furthermore, an innovative model originally developed for traditionally extruded components was implemented in a customized Fortran post-processing routine to investigate and predict the recrystallization behavior in the FSE of AA6061 aluminum alloy.

Introduction

In recent years, the European Commission has been actively pursuing sustainable growth strategies with a focus on competitive energy resources, taking into account both environmental impact and economic considerations [1]. A significant aspect of this endeavor involves addressing the challenges associated with the extensive waste generated by mechanical processes in industries such as metalworking. Conventional recycling methods often lead to increased energy consumption and difficulties in maintaining the desired alloy composition [2,3].

To overcome these challenges, the Welding Institute introduced Friction Stir Extrusion in 1993 as a novel metal shavings recycling process. FSE, characterized by solid-state recycling and high energy efficiency, has emerged as a promising technology, utilizing friction-generated heat for plastic deformation and extrusion of metal chips [4]. This process has demonstrated a remarkable reduction in energy consumption, requiring less than 15% of the energy used in conventional aluminum alloy melting processes [5]. In parallel with these advancements, it has become apparent that a crucial factor in optimization is understanding the intricate relationship between process parameters and the resulting physical outcomes [6]. Furthermore, the extrusion industry has long acknowledged the substantial attention given to the microstructure of aluminum alloy extruded profiles. The complex connection between process parameters and the evolution of grain structure presents challenges for extrusion companies striving to enhance product performance. So far, the scientific community has been actively engaged in investigating the recrystallization of aluminum

Content from this work may be used under the terms of the Creative Commons Attribution 3.0 license. Any further distribution of this work must maintain attribution to the author(s) and the title of the work, journal citation and DOI. Published under license by Materials Research Forum LLC.

alloys during the extrusion process. Efforts have been directed towards developing reliable models for recrystallization prediction, essential for controlling the final microstructure at the die design stage without costly experimental trial and error [6,7].

In the traditionally extruded pieces, the recrystallized structure, characterized by equiaxed grains, offers an avenue for optimizing product performance if appropriately controlled. Two main recrystallization mechanisms, dynamic recrystallization (DRX) and static recrystallization (SRX), have been identified, each influencing the microstructure during and after the extrusion process [8,9]. Despite numerous studies on recrystallization kinetics, limitations persist in the validation of models against industrial-scale extrusions with complex geometry profiles.

In response to this gap, this paper investigates the FSE process considering an already developed and optimized Finite Element simulation performed within the DEFORM™ 3D code. This model explores the influence of rotational tool speed and descent speed on process conditions, such as attained temperatures and the final volume of the workpiece. Additionally, stress conditions resulting from the simulations were analyzed using the Piwnik and Plata criterion to investigate the bonding phenomenon [10]. The study also aims to provide a comprehensive understanding of the recrystallization mechanisms involved. A recrystallization model, originally developed and validated for the traditional extrusion process [11], has been adapted for the FSE process. The ultimate objective is to propose a reliable model capable of accurately predicting the microstructural behavior in the AA6061 aluminum alloy Friction Stir Extruded (FSEed) profiles.

Procedure

A 3D Finite Element Lagrangian model was created using DEFORM™ 3D software to simulate the extrusion process. The tool and container were modeled as rigid bodies using AISI-1043 steel, while the aluminum scraps were treated as a porous workpiece of Aluminum-6061. The initial compaction phase was excluded for computational efficiency, and the initial density was set to 78% of the base aluminum, based on experimental tests, as also reported in [12–14]. Material flow stress data were sourced from the DEFORM™ 3D library for aluminum and steel, following both the law reported in Eq. 1.

$$\bar{\sigma} = \bar{\sigma}(\bar{\varepsilon}, \dot{\bar{\varepsilon}}, \mathrm{T}) \tag{1}$$

The steel tool and container were considered rigid due to the significant difference in yield strength compared to aluminum. The porous workpiece was meshed with 50,000 tetrahedral elements (Fig. 1).

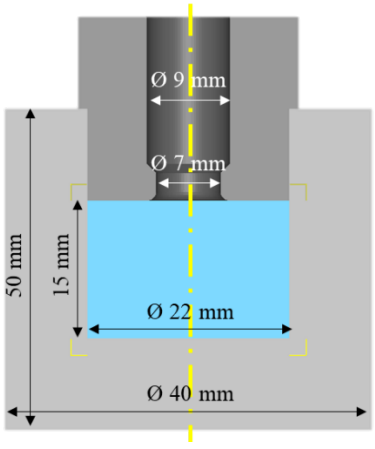

Figure 1: Geometry of the all simulated structure.

Thermal parameters were kept constant (Table 1), and simulations were conducted by varying tool rotational speed and descent speed to understand the bonding phenomenon (Table 2). The stop criterion was a tool displacement of 5 mm in the –Z direction.

Table 1: Thermal parameters used in the simulations [12].

Parameters	Value
Friction coefficient aluminum-tool	0.60
Thermal conductivity [N/(mm·s·°C)]	450
Aluminum emissivity	0.25
Heat transfer coefficient aluminum-tool [N/(mm·s·°C)]	11.00
Heat exchange with the environment [N/(mm·s·°C)]	0.02
Mechanical conversion to heat	0.80

Table 2: Combinations between the rotational speed (S) and the descent speed (F) considered for the simulations [12].

Combination	Rotational speed (S) [rpm]	Descent speed (F) [mm/s]
#1	400	1
#2	400	3
#3	800	1
#4	800	3

According to Piwnik and Plata criterion, material bonding is established when the parameter w, characterized as the integrated ratio over time between the pressure and the effective stress exerted on the material, attains a predetermined threshold value known as w_{lim}. This threshold is determined as a function of the temperature. To compute w and w_{lim} for every node at each step, a dedicated Fortran routine was specifically created and integrated into the simulation model. This ensured the automated calculation of these parameters and their relationship within the model. Moreover, a novel model initially designed for conventionally extruded components was incorporated into a tailored Fortran post-processing routine. This adaptation aimed to explore and anticipate the recrystallization behavior during the FSE of AA6061 aluminum alloy.

Modeling

The recrystallization model was taken from the work of Negozio et al. [15]. In this study, the model was developed and implemented in a subroutine for the assessment of dynamic and static recrystallization in post-processing to the Finite Element Method simulation of the extrusion process. To assess the microstructural evolution, the calculation of the Zener-Hollomon Z and sub-grain size δ parameters was carried out according to [16].

$$Z = \dot{\varepsilon}\, exp\left(\frac{Q}{RT}\right) \tag{2}$$

$$\frac{1}{\delta} = C\,(lnZ)^n \tag{3}$$

where $\dot{\varepsilon}$ is the maximum strain rate reached by each point during the investigated plastic deformation process, T is the temperature, n=5.577, C=3.36x10^{-9} m^{-1}, Q is the activation energy of the AA6061 aluminum alloy (196000 J/mol*K [17]), R is the universal gas constant (8.341 J/mol).

The energy responsible for activating the kinetics of static recrystallization is referred to as Stored Energy Pd and is calculated in accordance with [6]:

$$\mathrm{Pd} = \frac{Gb^2}{10}\left[\rho_i(1\text{-}\ln(10b\rho_i^{0,5}))+\frac{2\theta}{b\delta}*\left(1+\ln\left(\frac{\theta c}{\theta}\right)\right)\right] \tag{4}$$

where b the Burgers vector ($2.86x10^{-10}$ m [18]), G is the material shear modulus ($2.05x10^{10}$ Pa [18]), ρ_i the dislocation density, δ the sub-grain size, Θ the misorientation angle and Θc the misorientation angle limit (15°) [15].

The experimental analysis revealed a completely fibrous microstructure, without showing evidence of static recrystallization. Dynamic recrystallization modeling was conducted following the guidelines provided in [15]. The evolution of the grain size subjected to deformation was described based on the definition of two quantities, d_t (grain thickness) and d_l (grain length). These quantities were calculated as follows [15]:

$$d_t = (d_0 - 2.5\delta_{ss})(k_1)^{\bar{\varepsilon}} + 2.5\delta_{ss} \quad (5)$$

$$d_l = k_2\bar{\varepsilon}^2 - k_3\bar{\varepsilon} + d_0 \qquad \text{if } \varepsilon < \varepsilon_p \quad (6)$$

$$d_l = k_4\bar{\varepsilon}^{-m} + 10\delta_{ss} \qquad \text{if } \varepsilon > \varepsilon_p \quad (7)$$

where ε_p is the critical strain level for the pinch-off occurrence [17], which is considered as value of 3 [19], δ_{ss} is the subgrain size at the steady-state condition ($\delta_{ss} = 8.4$ µm) [19]) and m, k_1, k_2, k_3, k_4 are material constants identified in [19] as $m = 4.75, k_1 = 0.4, k_2 = 85.192, k_3 = 14.88, k_4 = 1.68 * 10^5$.

Results and discussion

When the occurrence of bonding according to the Piwnik and Plata criterion is verified, the Fortran variable named "Welding" shifts from 0 to 1. In such cases, the element undergoing this condition is visually highlighted in red. Conversely, blue indicates regions where stress conditions and temperature distribution are insufficient for the bonding of scraps. This approach facilitates pinpointing the occurrence and location of material bonding, as depicted in Fig. 2.

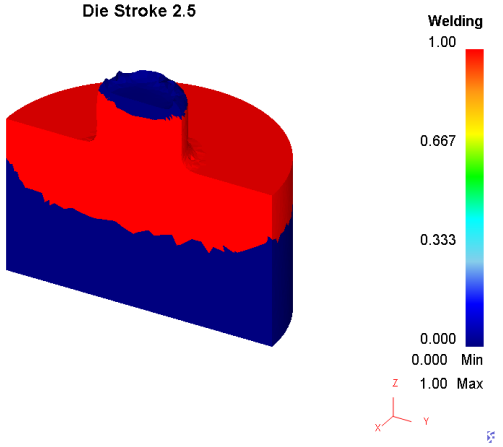

Figure 2: Red and blue areas in the FSEed object obtained with S=800 rpm, F=1 mm/s and Z=2.5 mm.

The examination of the simulation results revealed three global conditions: bonding, non-bonding, and limit conditions, across various combinations of operational parameters. Differentiating between instances where metal scraps have achieved complete bonding and cases where bonding was not accomplished before extrusion is crucial. This distinction is essential not only for identifying the presence of defects or voids within the extruded object but also for ensuring a comprehensive understanding of the bonding process. The limit condition involves the simultaneous presence of fully bonded material and still-porous metal scraps: this condition allows

for the production of extruded pieces with a solid external surface but internal sections of unbounded material. Identifying this scenario is essential, as it could lead to significant issues, resulting in a more fragile behavior than a completely solid FSEed sample.

Addressing these challenges requires precise definition of the boundary condition zone and the selection of parameter combinations guaranteed to fall within this range. This determination is facilitated by consulting the diagram presented in Fig. 3, which illustrates the summarized experimental results in terms of bonded and non-bonded specimens. The red cross designates the non-bonding zone, the green dot signifies the bonding zone, and the yellow triangle represents the limit condition zone.

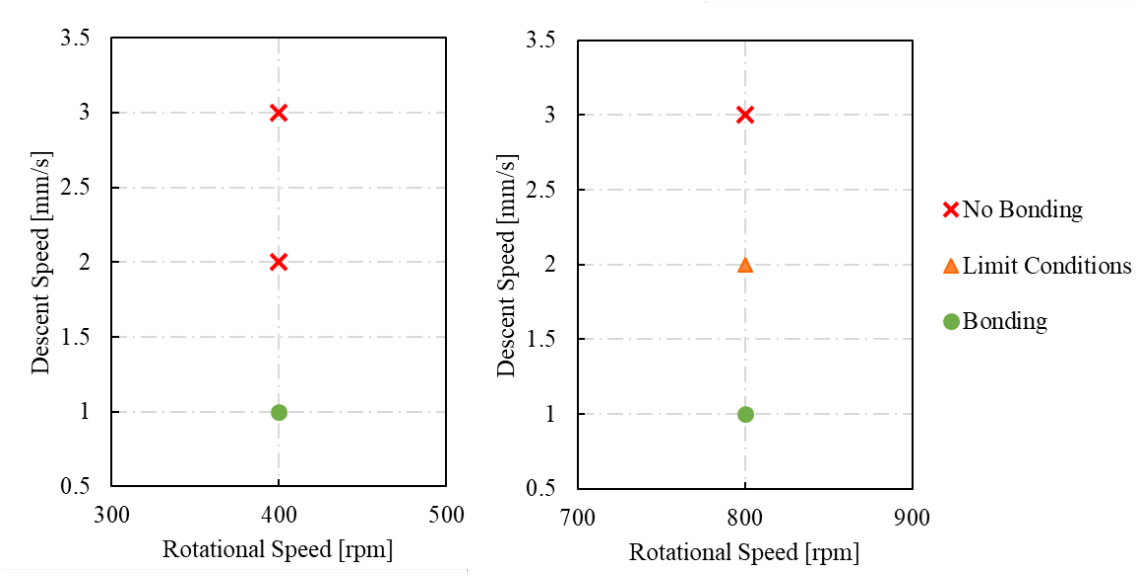

Figure 3: Bonding conditions as a function of the process parameters.

From the simulations point of view, the bonding, no bonding and limit conditions are reported in Fig. 4. The scenario where metal scraps are fully bonded (Fig. 4a) contrasts notably with instances where bonding fails to occur before extrusion (Fig. 4c).

An intermediate state, denoted henceforth as the limit condition entails a mixture of fully bonded material and still-porous metal scraps (Fig. 4b). In this state, extruded pieces may exhibit an exterior of solid material while retaining internal sections lacking bonding. Failure to detect this condition promptly could result in significant issues, as extruded pieces may demonstrate considerably reduced structural integrity compared to fully solid samples.

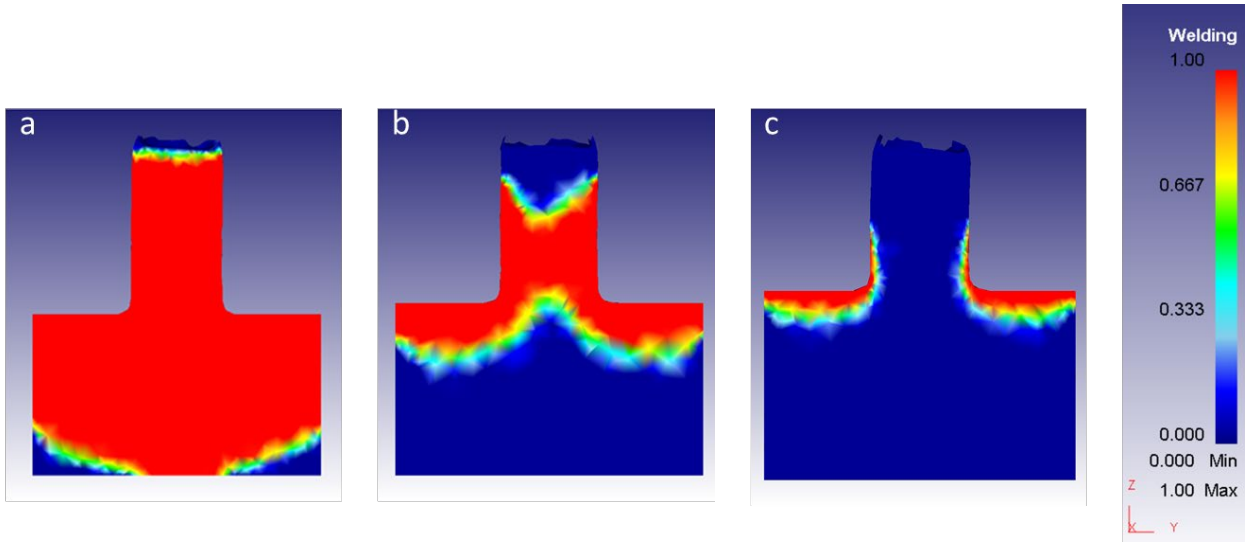

Figure 4: Different bonding conditions: (a) Completely bonded with S=800 rpm and F= 1 mm/s, (b) Limit condition with S=800 rpm and F= 2 mm/s and (c) Completely not bonded with S=800 rpm and F= 3 mm/s.

As already explained, the microstructure of aluminum alloy extruded profiles has garnered significant attention within the extrusion industry. For this reason, an additional Fortran routine was implemented in the post-processing phase within DEFORM™ 3D software. This routine, already developed for the traditional extrusion process and using Qform Extrusion software, was adapted to this new technology and this different software. With the revised routine, the possibility to foresee the medium grain dimension independently from the considered aluminum alloy was confirmed. Moreover, the prediction of the final grain dimensions is also possible to be achieved regardless of the size of the initial grains. Indeed, it is sufficient to modify only the parameters relative to the initial dimensions of the grain (also the longitudinal and transverse ones, if the starting material has no equiaxed grains). This allows the model to be adapted to the starting material, be it in the form of chips, powder or flat material by changing only the relevant variables first in the simulation model, mainly the starting density and the aluminum alloy, and the parameters mentioned above in the post-processor prediction model.

In the analyzed case, metal chip was considered as the starting material. Because of the small size and the machining operations that contributed to the formation of this chip, it is possible to think of it as consisting of rather uniform and equiaxial grains. For this reason, only the grain thickness will be plotted. Plotting this information within the routine, the microstructural trend of the extruded sample was evaluated by FSE. At the 5-mm end of the primary die run, a distinct grain refinement can be observed, as can be seen in Fig. 5. The trend of grain evolution and the results obtained were in line with what can be found in the literature. In particular, Buffa et al., obtained comparable results considering the same starting alloy, in the form of chips and the same rotational speed, showing that, from the microstructure point of view, no great differences were shown as a function of the different force applied in the tool thrust phase (Fig. 6), comparable in our case to the different tool descent speeds considered [20].

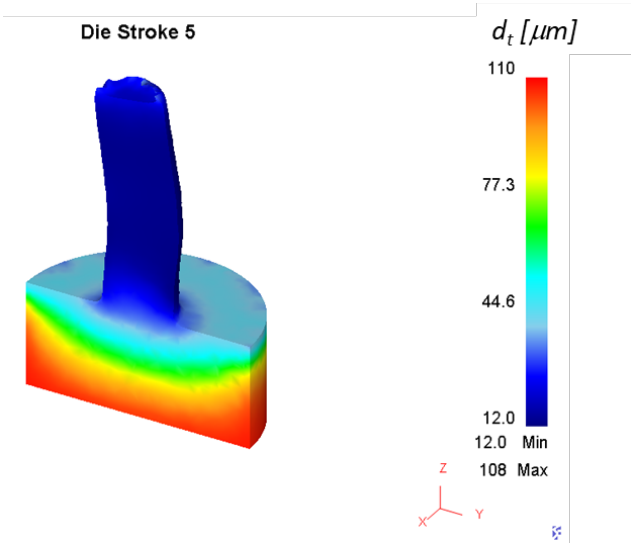

Figure 5: Grain dimensions in the FSEed sample obtained with S800 rpm and F=1 mm/min.

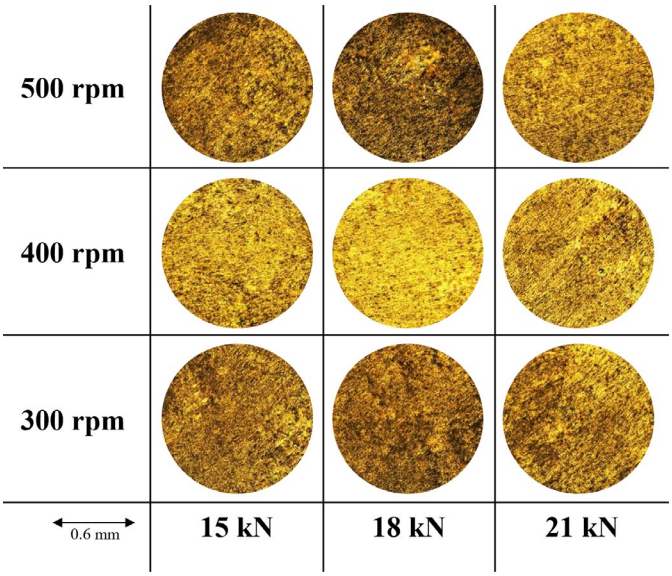

Figure 6: Etched cross sections of the AA6082 FSEed samples obtained with rotational speeds varying between 300 and 500 rpm and applied forces between 15 and 21 kN [20].

The grain sizes obtained, around 15-30 μm in the fully extruded part, are also consistent with what can be found in the literature [21]. Nevertheless, the proposed predictive model was also able to predict the trend of the average grain size within the extruded pieces. This is demonstrated by the images shown in Fig. 7, in which the close-up of the results obtained by applying the developed routine to the proposed simulation model is compared with the result obtained for the Friction Stir Consolidation process, which is a very similar process to the FSE process, except for the presence of the hole in the primary die [22].

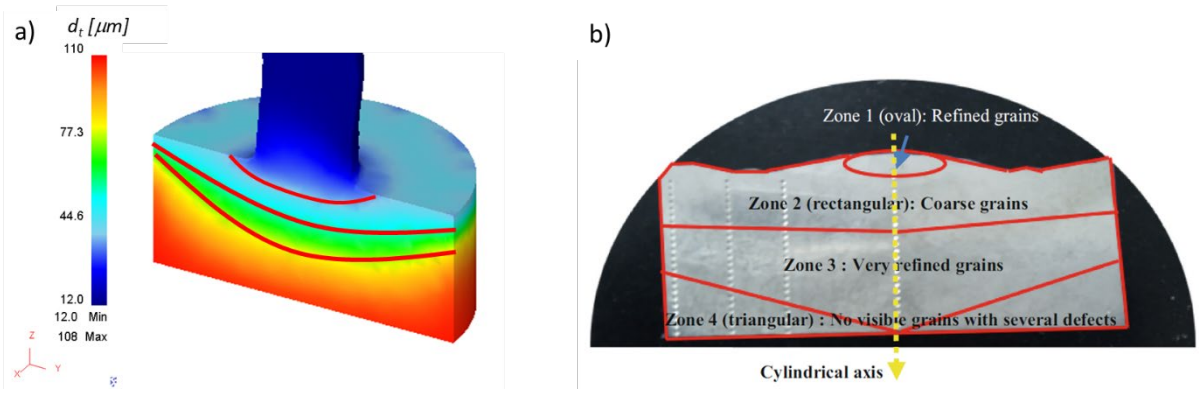

Figure 7: a) Close-up of the mean grains dimension of the compacted scraps reported in Figure 4. b) Grain characteristics obtained in a typical compacted workpiece obtained with the Friction Stir Consolidation (a very smilar process [22].

Conclusions

In the present work, a comprehensive understanding of the recrystallization mechanisms involved in the FSE process was carried out together with the FE simulation using DEFORM™ 3D code.

The main outcomes of this work are summarized as follows:

- The configuration of the Finite Element model offers an accurate forecast of the FSE physic.
- Piwnik and Plata criterion has demonstrated its effectiveness in accurately predicting the occurrence of bonding phenomena and understanding the impact of process parameters on the quality of produced parts.
- An innovative AA6061 recrystallization model originally developed to investigate the microstructure evolution in conventional extruded profiles proved to be suitable also for the FSE process.

Future developments of this research work will have as a central focus the further experimental validation of the simulative results obtained, with particular attention to the analysis of the effect of process parameters on the bonding conditions of the obtained extruded pieces.

References

[1] Brand U, Lang M. Green Economy Update Green Economy Update. vol. 1. Cheltenham/Northampton: Edward Elgar; 2015.

[2] Baffari D, Buffa G, Campanella D, Fratini L, Reynolds AP. Process mechanics in Friction Stir Extrusion of magnesium alloys chips through experiments and numerical simulation. J Manuf Process 2017;29:41–9. https://doi.org/10.1016/j.jmapro.2017.07.010

[3] Baffari D, Buffa G, Campanella D, Fratini L. Al-SiC Metal Matrix Composite production through Friction Stir Extrusion of aluminum chips. Procedia Eng., vol. 207, Elsevier B.V.; 2017, p. 419–24. https://doi.org/10.1016/j.proeng.2017.10.798

[4] Manchiraju K. Direct Solid-State Conversion of Recyclable Metals and Alloys. Golden, CO (United States): Southwire Company; 2012. https://doi.org/10.2172/1039705

[5] Izatt RM. Metal Sustainability: Global Challenges, Consequences, and Prospects. Wiley; 2016. https://doi.org/10.1002/9781119009115

[6] Donati L, Reggiani B, Pelaccia R, Negozio M, Di Donato S. Advancements in extrusion and drawing: a review of the contributes by the ESAFORM community. Int J Mater Form 2022;15:1–28. https://doi.org/10.1007/s12289-022-01664-w

[7] Zhang C, Wang C, Zhang Q, Zhao G, Chen L. Influence of extrusion parameters on microstructure, texture, and second-phase particles in an Al-Mg-Si alloy. J Mater Process Technol 2019;270:323–34. https://doi.org/10.1016/j.jmatprotec.2019.03.014

[8] Zhang C, Wang C, Guo R, Zhao G, Chen L, Sun W, et al. Investigation of dynamic recrystallization and modeling of microstructure evolution of an Al-Mg-Si aluminum alloy during high-temperature deformation. J Alloys Compd 2019;773:59–70. https://doi.org/10.1016/j.jallcom.2018.09.263

[9] Zhang T, Li L, Lu S, Li Z, Chen P, Gong H. Static recrystallization kinetics and microstructure evolution of 7055 aluminum alloy. Metall Res Technol 2019;116:120. https://doi.org/10.1051/metal/2018046

[10] Plata M, Piwnik J. Theoretical and experimental analysis of seam weld formation in hot extrusion of aluminum alloys. 7th Int. Alum. Extrus. Technol., 2000, p. 205–11.

[11] Negozio M, Donati L, Pelaccia R, Reggiani B, Di Donato S. Experimental analysis and modeling of the recrystallization behaviour of a AA6060 extruded profile. Mater. Res. Proc., vol. 28, Association of American Publishers; 2023, p. 477–86. https://doi.org/10.21741/9781644902479-52

[12] Bocchi S, D'urso G, Giardini C, Maccarini G. A Simulative Method for Studying the Bonding Condition of Friction Stir Extrusion. Key Eng Mater 2022;926 KEM:2333–41. https://doi.org/10.4028/P-FT5355

[13] Bocchi S, D'Urso G, Giardini C. Simulative Model for the Feasibility Study and Stress Analysis of Full Dense Rods and Pipes Produced by Friction Stir Extrusion. Lect. Notes Mech. Eng., 2024, p. 398–406. https://doi.org/10.1007/978-3-031-41023-9_41

[14] Bocchi S, D'Urso G, Giardini C. Numerical Modeling of a Sustainable Solid-State Recycling of Aluminum Scraps by Means of Friction Stir Extrusion Process. Materials (Basel) 2023;16:4375. https://doi.org/10.3390/ma16124375

[15] Negozio M, Pelaccia R, Donati L, Reggiani B. Simulation of the microstructure evolution during the extrusion of two industrial-scale AA6063 profiles. J Manuf Process 2023;99:501–12. https://doi.org/10.1016/j.jmapro.2023.05.075

[16] Negozio M, Pelaccia R, Donati L, Reggiani B. Numerical investigation of the surface recrystallization during the extrusion of a AA6082 aluminum alloy under different process conditions. Int J Adv Manuf Technol 2023;129:1585–99. https://doi.org/10.1007/s00170-023-12397-8

[17] Khamei AA, Dehghani K, Mahmudi R. Modeling the hot ductility of AA6061 aluminum alloy after severe plastic deformation. JOM 2015;67:966–72. https://doi.org/10.1007/s11837-015-1354-3

[18] Vatne HE, Furu T, Ørsund R, Nes E. Modelling recrystallization after hot deformation of aluminium. Acta Mater 1996;44:4463–73. https://doi.org/10.1016/1359-6454(96)00078-X.

[19] Donati L, Segatori A, El Mehtedi M, Tomesani L. Grain evolution analysis and experimental validation in the extrusion of 6XXX alloys by use of a lagrangian FE code. Int J Plast 2013;46:70–81. https://doi.org/10.1016/j.ijplas.2012.11.008

[20] Buffa G, Campanella D, Adnan M, La Commare U, Ingarao G, Fratini L. Improving the Industrial Efficiency of Recycling Aluminum Alloy Chips Using Friction Stir Extrusion: Thin

Wires Production Process. Int J Precis Eng Manuf Technol 2024. https://doi.org/10.1007/s40684-023-00573-w

[21] Chan CYC, Rath L, Suhuddin UFH, Klusemann B. Friction extrusion processing of aluminum powders: Microstructure homogeneity and mechanical properties. Mater. Res. Proc., vol. 28, Association of American Publishers; 2023, p. 515–22. https://doi.org/10.21741/9781644902479-56

[22] Latif A, Gucciardi M, Ingarao G, Fratini L. Outlining the Limits of Friction Stir Consolidation as Used as an Aluminum Alloys Recycling Approach. Smart Innov. Syst. Technol., vol. 262 SIST, Springer Science and Business Media Deutschland GmbH; 2022, p. 169–80. https://doi.org/10.1007/978-981-16-6128-0_17